Letter

Nucleon sigma terms with a variational analysis from Lattice QCD

Lorenzo Barca,[1,*] Gunnar Bali,[2,†] and Sara Collins[2,‡]

[1]*John von Neumann-Institut für Computing (NIC), Deutsches Elektronen-Synchrotron (DESY), Platanenallee 6, 15738 Zeuthen, Germany*

[2]*Fakultät für Physik, Universität Regensburg, Universitätsstraße 31, 93053 Regensburg, Germany*

(Received 18 December 2024; accepted 9 January 2025; published 25 February 2025)

We determine the nucleon-sigma terms from lattice quantum chromodynamics (QCD). We find that the dominant excited state contamination in the nucleon three-point function with a scalar current is due to the transition between the nucleon and a S-wave scattering state of a nucleon and a scalar (sigma) meson. In this proof-of-concept study, we analyze a single $N_f = 3$ ensemble with the unphysically large pion mass $M_\pi = 429$ MeV. Excited state contamination is substantially reduced compared to the standard method when employing nucleon-sigma type interpolating operators within a generalized eigenvector analysis.

DOI: 10.1103/PhysRevD.111.L031505

Introduction. Almost all visible matter of the Universe is composed of nucleons, i.e. protons and neutrons. Most of the nucleons' mass can be attributed to the spontaneous breaking of chiral symmetry. Only a small part is due to the Higgs mechanism, i.e. the masses of the valence and sea quarks. These contributions can be quantified in a scheme- and gauge-invariant way in terms of scalar matrix elements, the quark-nucleon σ-terms,

$$\sigma_{qN} = m_q \langle N|\bar{q}q|N\rangle = m_q \frac{\partial m_{\rm N}}{\partial m_q}, \tag{1}$$

where $q \in \{u, d, s, \ldots\}$. These determine the coupling strength of the Standard Model Higgs boson (or other scalar particles) at zero recoil to the nucleon and are therefore important for theory predictions relevant for the direct detection of weakly interacting massive dark matter particles, see, e.g., the review [1].

In the isospin symmetric limit, i.e. for equal up and down quark masses $m_u = m_d$ and electric charges, the pion-nucleon σ-terms $\sigma_{\pi N} = \sigma_{uN} + \sigma_{dN}$ are the same for the proton and the neutron: $\sigma_{\pi p} = \sigma_{\pi n}$. $\sigma_{\pi N}$ can be extracted indirectly via dispersive analyses of pion-nucleon scattering data, employing low energy theorems and chiral perturbation theory (ChPT). Initially, a value $\sigma_{\pi N} = 45(8)$ MeV [2] was obtained. More recent phenomenological determinations, when corrected for isospin breaking effects [3], scatter around 56 MeV [3–7]. The σ-terms can also be determined from first principles lattice QCD, either directly [8–13] or indirectly [14–18] from the quark- (or the pseudoscalar meson mass-) dependence of the nucleon mass, using the second equality of Eq. (1). The most recent Flavour Lattice Averaging Group (FLAG) average of results obtained via the direct and the indirect methods, reads for the $N_f = 2 + 1$ theory $\sigma_{\pi N} = 42.2(2.4)$ MeV [19]. No tension is seen between the individual determinations. In contrast, the $N_f = 2 + 1 + 1$ average reads $\sigma_{\pi N} = 60.9(6.5)$ MeV [19]. This average, which is closer to the recent phenomenological estimates, is dominated by the PNDME result [11], obtained via the direct method.

Nucleon matrix elements, including the scalar matrix elements, are extracted from combinations of Euclidean two- and three-point functions. Within these, interpolating operators (interpolators) with the quantum numbers of the nucleon at a given three-momentum are used to create and to destroy hadronic states that propagate in Euclidean time. In the three-point function, a local quark bilinear current is inserted at an intermediate time. The interpolators not only create the ground state of interest but also excited states, including a tower of multiparticle states composed of a baryon and mesons. The ground state properties of interest can in principle be obtained in the limit of large Euclidean time separations between the "source," the current (in the case of three-point functions) and the "sink." Due to the exponential noise over signal problem of baryonic Green functions [20,21], excited state contributions are often still significant for the separations that are achievable within reasonable precision. These are then accounted for by carrying out multiexponential fits. Within three-point functions, the transitions between the ground and some excited states can be particularly enhanced since the current

*Contact author: lorenzo.barca@desy.de
†Contact author: gunnar.bali@ur.de
‡Contact author: sara.collins@ur.de

can directly create a meson which, in combination with a baryon, can give the quantum numbers of the final state nucleon. The transition from N states to $N\pi$ and $N\pi\pi$ states, mediated by a current, has been investigated using ChPT [11,22–25]. Results of such calculations have then inspired the fit *Ansätze* used in lattice analyses, e.g., of axial and pseudoscalar form factors [26,27] and σ-terms [11,12].

Motivated by ChPT, PNDME [11] constrain the gap between the ground and the first excited state energies to agree within 20% with the difference between the nucleon mass and the lowest possible noninteracting $N\pi$ (P-wave) or $N\pi\pi$ (S-wave) energy level. In their multistate analysis this has a large impact, in particular, at small pion masses and for the disconnected quark line Wick contraction, resulting in the final value $\sigma_{\pi N} = 59.6(7.4)$ MeV. This is larger than what was found in other recent direct determinations [8–10,12,13] or predictions using the indirect (Feynman-Hellmann) method [15–17], with different systematics related to excited states.

A more systematic approach would be to explicitly resolve and subtract the dominant excited state contributions using a variational approach with a basis of interpolators, including baryon-meson type operators. The efficacy of this approach was first demonstrated in [28] at unphysically large pion masses, where the contributions from the lowest $N\pi$ excited states were removed from axial and pseudoscalar three-point functions with and without momentum transfer.[1] Subsequently, in [29] this was confirmed at the physical pion mass and extended to vector, tensor and scalar matrix elements. In the latter case no improvement was found when adding the lowest P-wave nucleon-pion type operator to the interpolator basis. This may not be surprising since one would expect flavor-diagonal scalar currents to dominantly couple to isoscalar scalar meson resonances. At the physical point this would be the $f_0(500)$ (decaying into $\pi\pi$) and the $f_0(980)$. In terms of the flavour content, these are mixtures of the scalar $I = I_3 = S = 0$ singlet and octet SU(3) eigenstates σ_0 and σ_8, respectively.

Restricting ourselves to the baryon-(single)meson sector, a number of interpolators with the quantum numbers of a nucleon at rest can be constructed. These include P-wave combinations of type $N\pi$, $N\eta_0$, $N\eta_8$, ΣK etc. as well as S-wave combinations like Na_0, $N\sigma_0$, $N\sigma_8$, ΣK_0^* and so on. To resolve the dominant multiparticle excited state it may be sufficient just to employ interpolators containing flavour-diagonal scalar mesons since only these can be created directly by the $\bar{u}u + \bar{d}d$ and $\bar{s}s$ currents of interest. These are the σ_0 and σ_8 mesons with flavour content $(\bar{u}u + \bar{d}d + \bar{s}s)/\sqrt{3}$ and $(\bar{u}u + \bar{d}d - 2\bar{s}s)/\sqrt{6}$, respectively. In addition we consider a $N\sigma$ interpolator with $\sigma \sim (\bar{u}u + \bar{d}d)/\sqrt{2}$.

In this proof-of-concept study, we investigate whether excited state contamination for scalar matrix elements can indeed be reduced in a variational approach, including either $N\sigma$ or $N\sigma_0$ and $N\sigma_8$ type interpolators in the basis. This work is carried out on a single Coordinated Lattice Simulations [30] ensemble employing $N_f = 3$ nonperturbatively improved Wilson fermions at a larger than physical pion mass[2] $M_\pi \approx 429$ MeV on the SU(3) flavor symmetric line ($m_q = m_u = m_d = m_s$, i.e., $M_K = M_\pi$) and a lattice spacing $a \approx 0.098$ fm. For this quark mass combination the σ_0 meson is stable with the mass $M_{\sigma_0} = 554(49)$ MeV (see the Supplemental Material [31]), similar to the real part of the pole of the $f_0(500)$ observed in nature. We remark that the variational approach with a basis of N and $N\sigma$ type interpolators (along with, e.g., $N\pi$ interpolators) has been investigated previously in the context of scattering studies [32,33].

This letter is organized as follows. In Sec. II we introduce the general procedure for the direct determination of the renormalized σ-terms. We then detail our variational determination of the energy eigenvalues and eigenvectors in Sec. III and compare results from fits to the improved and standard Green's functions in Sec. IV, before we conclude in Sec. V.

Direct determination of the σ-terms. The scalar matrix elements can be extracted from two- and three-point functions

$$C_{\rm 2pt}(t) = \langle \mathrm{O}(t)\bar{\mathrm{O}}(0)\rangle, \tag{2}$$

$$C^{\mathcal{S}^q}_{\rm 3pt}(t,\tau) = \langle \mathrm{O}(t)\mathcal{S}^q(\tau)\bar{\mathrm{O}}(0)\rangle, \tag{3}$$

in the rest frame. The interpolating operator $\bar{\mathrm{O}}$ (O) creates (annihilates) states with the quantum numbers of the nucleon $I(J^P) = \frac{1}{2}(\frac{1}{2}^+)$ at the source on timeslice 0 (sink on timeslice t). For the three-point function, the scalar current $\mathcal{S}^q = \bar{q}q$ is inserted at an intermediate time τ, where we consider the flavour combinations $\mathcal{S}^{u+d} = \bar{u}u + \bar{d}d$ and $\mathcal{S}^s = \bar{s}s$. The spectral decomposition of the correlation functions reads

$$C_{\rm 2pt}(t) = \sum_n |Z_n|^2 e^{-E_n t}, \tag{4}$$

$$C^{\mathcal{S}^q}_{\rm 3pt}(t,\tau) = \sum_{n',n} Z_{n'}\bar{Z}_n \langle n'|\mathcal{S}^q|n\rangle e^{-E_{n'}(t-\tau)} e^{-E_n\tau}. \tag{5}$$

E_n is the energy of state $|n\rangle$, created by the interpolator $\bar{\mathrm{O}}$ from the vacuum state $|\Omega\rangle$, and $\bar{Z}_n$ is the associated overlap factor $\bar{Z}_n \propto \langle n|\bar{\mathrm{O}}|\Omega\rangle$. In the limit of large time separations

[1]No improvement was seen in the forward limit, in the rest frame.

[2]The trace of the mass matrix $m_u + m_d + m_s$ is close to that at the physical point.

$t \gg \tau \gg 0$, the ground state contribution ($n = n' = N$) dominates. By performing fits to combinations of the two- and three-point functions (see Sec. IV) the nucleon scalar matrix elements in the lattice scheme can be extracted

$$\langle N|\mathcal{S}^{u+d}|N\rangle = \bar{u}_N g_S^{\mathrm{lat},u+d} u_N, \tag{6}$$

$$\langle N|\mathcal{S}^{s}|N\rangle = \bar{u}_N g_S^{\mathrm{lat},s} u_N. \tag{7}$$

The Lorentz decomposition of these matrix elements is expressed in terms of the scalar charges $g_S^{\mathrm{lat},q}$, $q \in \{u, d, s\}$, and u_N, the spinor of a nucleon at rest. For Wilson fermions, on the SU(3) flavor symmetric line the renormalized σ-terms are given by

$$\sigma_{\pi N} = m_q \left[r_m g_S^{\mathrm{lat},u+d} + \frac{2}{3}(1 - r_m) g_S^{\mathrm{lat},u+d+s} \right], \tag{8}$$

$$\sigma_{sN} = m_q \left[r_m g_S^{\mathrm{lat},s} + \frac{1}{3}(1 - r_m) g_S^{\mathrm{lat},u+d+s} \right], \tag{9}$$

where m_q is the vector Ward identity quark mass and r_m is the ratio of the singlet to nonsinglet mass renormalization factors. In our case, $r_m = 3.409(57)$ [34] and $m_q = 6.62(25)$ MeV [17].

Variational analysis. To construct an interpolator with large overlap to the nucleon ground state, we perform a variational analysis [35]. We utilise two bases of interpolators with proton quantum numbers ($I_z = +1/2$). Basis $\mathbb{B}_2 = \{\mathrm{O}_p, \mathrm{O}_{p\sigma}\}$ comprises the usual proton interpolator $\mathrm{O}_p = u^T(dC\gamma_5 u)$ and a S-wave proton-sigma meson interpolator $\mathrm{O}_{p\sigma}$, combining O_p with the SU(2) sigma meson operator ($I = 0$, $J^{PC} = 0^{++}$), $\mathrm{O}_\sigma = (\bar{u}u + \bar{d}d)/\sqrt{2}$. For basis $\mathbb{B}_3 = \{\mathrm{O}_p, \mathrm{O}_{p\sigma_0}, \mathrm{O}_{p\sigma_8}\}$, we implement the SU(3) singlet and octet sigma meson operators, $\mathrm{O}_{\sigma_0} = (\bar{u}u + \bar{d}d + \bar{s}s)/\sqrt{3}$ and $\mathrm{O}_{\sigma_8} = (\bar{u}u + \bar{d}d - 2\bar{s}s)/\sqrt{6}$, respectively. To improve the overlap with lower-lying levels, we construct spatially extended interpolators by Wuppertal smearing [36,37] the quark fields, incorporating APE smeared links [38]. For the nucleon and σ operators within the single- and two-hadron interpolators we employ the smearing radii $\langle r^2\rangle^{1/2} \sim 1.0$ fm and $\langle r^2\rangle^{1/2} \sim 0.2$ fm, respectively.

Using these bases, we build the following matrices of two-point functions

$$\mathbb{C}_{2\mathrm{pt}}(t)_{ij} = \langle \mathrm{O}_i(t)\bar{\mathrm{O}}_j(0)\rangle \tag{10}$$

with $\mathrm{O}_i, \mathrm{O}_j \in \mathbb{B}_2$ or $\mathbb{B}_3$. The corresponding Wick contractions are evaluated using the sequential source method [39] for quark-line connected topologies. For the disconnected diagrams also stochastic estimation is used, including the one-end-trick [40,41], see the Supplemental Material [31]. We solve the generalized eigenvalue problem (GEVP)

$$\mathbb{C}_{2\mathrm{pt}}(t)V(t,t_0) = \mathbb{C}_{2\mathrm{pt}}(t_0)V(t,t_0)\Lambda(t,t_0) \tag{11}$$

for different reference times t_0 and $t > t_0$. This gives the matrix of generalized eigenvalues $\Lambda(t,t_0) = \mathrm{diag}(\lambda^\alpha(t,t_0))$ and eigenvectors $V(t,t_0) = (v_i^\alpha(t,t_0))$, where the superscripts (subscripts) refer to the eigenstate (operator) and we employ the normalization $v^{\alpha\intercal}\mathbb{C}_{2\mathrm{pt}}(t_0)v^\beta = \delta^{\alpha\beta}$. In the limit of large times, the eigenvalues decay exponentially with the energy of the state, $\lambda^\alpha(t,t_0) \propto e^{-E_\alpha(t-t_0)}$, while the elements of the eigenvectors $v_i^\alpha(t,t_0)$ are related to the overlap of the operator O_i with the state α.

The effective energies $E_{\mathrm{eff}}^\alpha(t) = a^{-1}\ln[\lambda^\alpha(t)/\lambda^\alpha(t+a)]$ are shown in Fig. 1 for $t_0 = 0.3$ fm.[3] For both bases, the lowest energy coincides with the nucleon mass on this ensemble [17], while the second level is close to the sum of the nucleon and sigma energies. Therefore, we will identify $\alpha = 1$ with N and $\alpha = 2$ with $N\sigma$. The third eigenvalue for basis $\mathbb{B}_3$ does not exhibit a clear plateau, with the statistical errors increasing rapidly for $t - t_0 - a > 3a$. We were not able to obtain a reliable estimate of the σ_8 meson mass, however, assuming the masses of the σ_8 and the physical $f_0(980)$ are similar [as is the case for σ_0 and $f_0(500)$], the $N\sigma_8$ noninteracting level would lie around 2200 MeV, above the almost degenerate lowest P-wave $N\pi$ and S-wave $N\pi\pi$ levels.

We observe that $E_{\mathrm{eff}}^1(t)$ is consistent with the effective mass of the standard nucleon two-point function, $C_{2\mathrm{pt}}^{\mathrm{STD}}(t) = \mathbb{C}_{2\mathrm{pt}}(t)_{11} = \langle \mathrm{O}_p(t)\bar{\mathrm{O}}_p(0)\rangle$, see Fig. 1, which plateaus already at $t = 0.5$ fm (equal to $t - t_0 - a = a$ for $t_0 = 3a$).

The multiparticle interpolators contribute two orders of magnitude less to v^1 than O_p, however, the impact on three-point functions can still be significant, see below. Note that the O_p contribution also dominates v^2 (and v^3).

An operator with an improved overlap to the ground state can be constructed from a linear combination of the initial operators O_i and the eigenvectors for the first level $v_i^{\alpha=1}(t',t_0)$ evaluated at a large enough time t' such that the eigenvector is stable ($t \geq t' = 6a$ for $t_0 = 3a$ in our setup),

$$\mathrm{O}^{\mathrm{imp}}(t) \propto \sum_{i\in\mathbb{B}} v_i^{\alpha=1}(t',t_0)\mathrm{O}_i(t - t_0/2), \tag{12}$$

with $\mathbb{B} = \mathbb{B}_2$ or $\mathbb{B}_3$. This operator can be used to define GEVP-improved two- and three-point functions

[3]This value of t_0 proved the best choice for our setup in terms of resolving the lowest two states and minimizing the statistical noise.

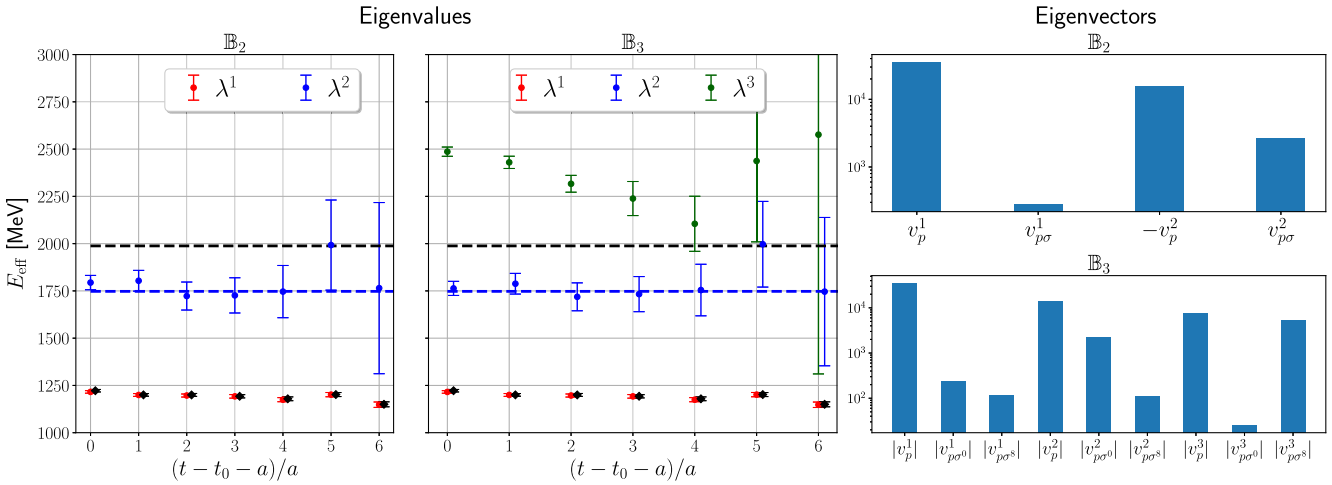

FIG. 1. Effective energies obtained from the GEVP with interpolator bases $\mathbb{B}_2$ (left) and $\mathbb{B}_3$ (middle) for $t_0 = 3a$, compared to the effective mass of the standard nucleon two-point function (black diamonds) constructed from the O_p operators. The dashed lines correspond to the energies of the noninteracting S-wave $N\sigma$ (blue) and lowest P-wave $N\pi$ (black) levels. Also shown are the corresponding generalized eigenvector components for $t - t_0 = 3a$ for $\mathbb{B}_2$ (right top) and $\mathbb{B}_3$ (right bottom).

$$C_{\rm 2pt}^{\rm imp}(t) = \langle \mathrm{O}^{\rm imp}(t)\bar{\mathrm{O}}^{\rm imp}(0)\rangle, \tag{13}$$

$$C_{\rm 3pt}^{{\rm imp},\mathcal{S}^q}(t,\tau) = \langle \mathrm{O}^{\rm imp}(t)\mathcal{S}^q(\tau)\bar{\mathrm{O}}^{\rm imp}(0)\rangle. \tag{14}$$

We neglect the $N\sigma \xrightarrow{\mathcal{S}^q} N\sigma$ contributions to $C_{\rm 3pt}^{{\rm imp},\mathcal{S}^q}$ that are suppressed by the second power of the small eigenvector component $v_{p\sigma}^1$ for $\mathbb{B}_2$ ($v_{p\sigma_0,p\sigma_8}^1$ for $\mathbb{B}_3$). In particular, we do not expect the matrix element $\langle N\sigma|\mathcal{S}^q|N\sigma\rangle$ to be enhanced relative to $\langle N|\mathcal{S}^q|N\rangle$. In order to assess the size of excited state contamination to the improved three-point function we form the ratio

$$R_{u+d,s}^{\rm GEVP}(t,\tau) = \frac{C_{\rm 3pt}^{{\rm imp},\mathcal{S}^{u+d,s}}(t,\tau)}{C_{\rm 2pt}^{\rm imp}(t)} \tag{15}$$

for the $\mathcal{S}^{u+d}$ and $\mathcal{S}^s$ currents for 10 source-sink separations, $t = 2a - 11a = 0.2$–1.1 fm, shown in Fig. 2. Considering the spectral decomposition given in Sec. II, this ratio tends to the charges $g_S^{{\rm lat},u+d}$ and $g_S^{{\rm lat},s}$ of the nucleon, respectively, at large time separations. For comparison we also evaluate $R_{u+d,s}^{\rm STD}(t,\tau)$, the ratio of the standard three-point function $C_{\rm 3pt}^{\rm STD}(t,\tau) = \langle \mathrm{O}_p(t)\mathcal{S}^{u+d,s}(\tau)\bar{\mathrm{O}}_p(0)\rangle$ to $C_{\rm 2pt}^{\rm STD}(t)$ for $t = 2a - 17a = 0.2$–1.7 fm. Note that only the ratios up to $t = 14a$ are shown in the figure. The standard ratios show a significant dependence on the source-sink separation and current insertion time, indicating large excited state contributions to the three-point function. In contrast, the GEVP ratios display a much milder dependence. This suggests that the S-wave $N\sigma$ contributions to $C_{\rm 3pt}^{\rm STD}(t,\tau)$ are significant and that these are effectively removed when employing the GEVP-improved interpolator. However, clearly, residual excited state contamination remains and a larger basis of operators would need to be considered to reduce these contributions further.

Fitting analysis. In the following, we present the fitting analysis carried out to extract the scalar charges from the ratios of the three-point to two-point correlation functions. With a large number of source-sink separations (t) at our disposal, we employ the summation method and compute

$$R_{u+d,s}^{\rm sum}(t) = \sum_{\tau=+c}^{t-c} R_{u+d,s}(t,\tau), \tag{16}$$

where the sum over the current insertion (τ) runs from time slice $\tau = c$ up to $t - c$. Considering the spectral decompositions in Eqs. (4) and (5) truncated after the first excited state, the t-dependence of the summed ratio reads

$$R_{u+d,s}^{\rm sum}(t) = g_S^{{\rm lat},u+d,s}(t-2c+a) + 2c_{10}\frac{e^{\Delta E(c-t)} - e^{\Delta E(a-c)}}{1-e^{\Delta E}} + c_{11}(t-2c+a)e^{-\Delta E t}. \tag{17}$$

The coefficients c_{10} and c_{11} are related to the matrix elements $\langle N|\mathcal{S}^{u+d,s}|2\rangle$ and $\langle 2|\mathcal{S}^{u+d,s}|2\rangle$, respectively, and ΔE denotes the energy gap between the ground $|N\rangle = |1\rangle$ and the first resolvable excited state $|2\rangle$. In the limit of ground state dominance, this dependence simplifies to

$$R_{u+d,s}^{\rm sum}(t) = c_0 + g_S^{{\rm lat},u+d,s}t \tag{18}$$

with $c_0 = g_S^{u+d,s}(a-2c)$.

First, we discuss the fits to the standard ratios $R_{u+d,s}^{\rm STD}(t,\tau)$. Given the significant excited state contributions for smaller t seen in Fig. 2, we perform correlated fits

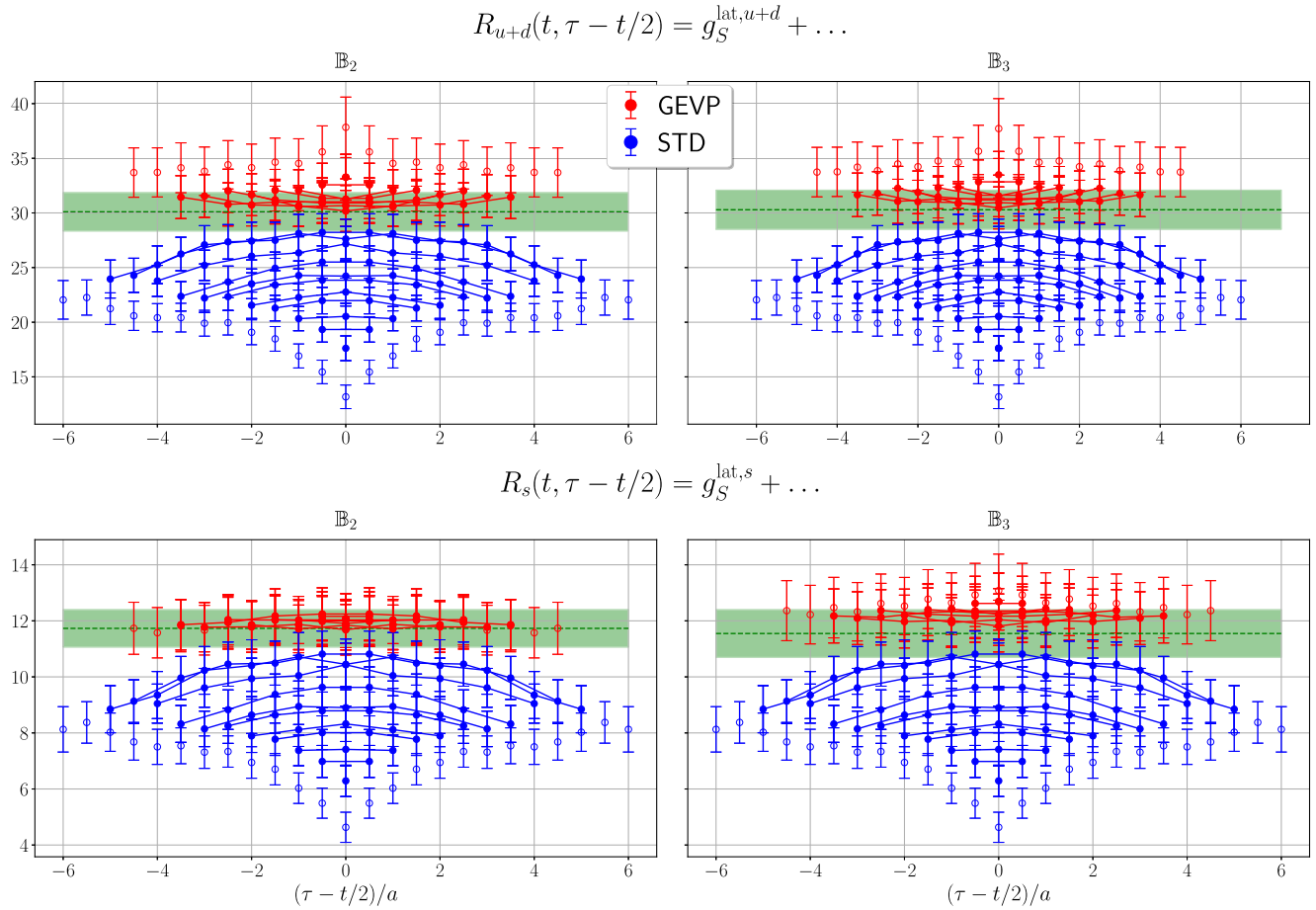

FIG. 2. Results for the GEVP-improved ratios R_{u+d} (top) and R_s (bottom) for $\mathbb{B}_2$ (left) and $\mathbb{B}_3$ (right). The green dashed lines and bands show the central values and errors, respectively, of $g_S^{\mathrm{lat},u+d}$ (top) and $g_S^{\mathrm{lat},s}$ (bottom) extracted using the summation method, see Sec. IV. The standard ratios obtained using the interpolator O_p are shown for comparison. The data points that are utilised in the fits (Sec. IV) are indicated by solid circles.

to the summed ratios employing Eq. (17) with $c = 2a$. The latter means that the summed ratio is realised for $t \geq 4a$. We set $c_{11} = 0$ as the term involving the excited-state to excited state transition was not resolved. The fit range is varied and we take a weighted average of the results.[4] The values obtained for $g_S^{u+d,s}$ and ΔE are listed in Table I. The energy gap is not well determined in the fits, however, we know from the GEVP analysis (see Fig. 1) that the first excited state energy is consistent with the S-wave $N\sigma$ noninteracting level. This motivates us to repeat the analysis imposing a prior on ΔE equal to the mass of the sigma meson with a width of 50 MeV (9%), leading to similar results for the scalar charges but with smaller uncertainties. In the absence of detailed knowledge of the energy spectrum, a prior for the energy gap is often set using the P-wave $N\pi$ energy (although additional excited states are usually taken into account in the fit model). A larger energy gap gives consistent but slightly lower values for the scalar charges. For $t \geq 8a$ we are also able to perform linear fits (18) (see Table I) since the excited state contributions to $R_{u+d,s}^{\mathrm{sum}}$ fall below the noise.

For completeness, we also carried out correlated fits to $R_{u+d,s}^{\mathrm{STD}}(t,\tau)$ with the following *Ansatz*:

$$R_{u+d,s}(t,\tau) = g_S^{\mathrm{lat},u+d,s} + c_{10}\left(e^{-\Delta E(t-\tau)} + e^{-\Delta E\tau}\right), \quad (19)$$

where, again, the excited-state to excited-state term is omitted. We simultaneously fit the ratios with $t/a = 8$, 9, 11, 13, 15 employing the fit range $2a \leq \tau \leq t - 2a$ for each t.[5] The largest source-sink separations are not included

[4]The weighted average $\bar{a}$ of fit coefficient $a \in \{g_S^{u+d,s}, \Delta E\}$ is computed using weights $w_i = N \exp\left(-(\chi_i^2 - \mathrm{N}_{\mathrm{df}\,i})/2\right)$, where χ_i^2 and $\mathrm{N}_{\mathrm{df}\,i}$ are the fit quality and number of degrees of freedom for fit i, respectively. N is chosen so that $\sum_i w_i = 1$. The average $\bar{a}$ and its uncertainty Δa are given by $\bar{a} = \sum_i w_i a_i$ and $\Delta a^2 = \sum_i w_i \Delta a_i^2$, where Δa_i is the bootstrapped error for fit i.

[5]For our setup, with 800 configurations employed in the analysis, this choice ensures that the covariance matrix is well determined.

TABLE I. Results for the unrenormalized nucleon scalar charges from the standard ratio $R^{\mathrm{STD}}_{u+d,s}(t,\tau)$. These and the summed ratios (16) are fitted according to Eqs. (19), (17), and (18), respectively. For the latter, the fit range is varied for each model and a weighted average is quoted, along with the range of the $\chi^2/\mathrm{N_{df}}$ Where applicable, the energy gaps ΔE between the first excited state and the ground state are given. Priors for ΔE based on the noninteracting S-wave $N\sigma$ or P-wave $N\pi$ energies are labelled as $\Delta E_{N\sigma}$ and $\Delta E_{N\pi}$, respectively, see the text.

Fit models	$g_S^{\mathrm{lat},u+d}$	ΔE [MeV]	$\chi^2/\mathrm{N_{df}}$	$g_S^{\mathrm{lat},s}$	ΔE [MeV]	$\chi^2/\mathrm{N_{df}}$
Eq. (17) ⌇ $c_{11}=0$	31.7 ± 2.6	495 ± 191	[1.1, 1.3]	11.8 ± 1.0	526 ± 193	[1.1, 1.3]
Eq. (17) ⌇ $c_{11}=0$, $\Delta E_{N\sigma}$	30.8 ± 1.8	516 ± 35	[1.1, 1.4]	11.7 ± 0.9	514 ± 33	[1.1, 1.3]
Eq. (17) ⌇ $c_{11}=0$, $\Delta E_{N\pi}$	29.0 ± 1.6	678 ± 31	[1.2, 1.5]	10.9 ± 0.8	678 ± 30	[1.2, 1.4]
Eq. (18)	30.0 ± 2.0		[1.0, 1.4]	11.6 ± 0.9		[0.9, 1.5]
Eq. (19)	31.8 ± 2.6	566 ± 132	0.63	12.3 ± 0.9	537 ± 114	0.61
Eq. (19) ⌇ $\Delta E_{N\sigma}$	31.6 ± 2.0	553 ± 52	0.63	12.2 ± 0.7	527 ± 40	0.61
Eq. (19) ⌇ $\Delta E_{N\pi}$	29.5 ± 1.6	690 ± 39	0.65	11.2 ± 0.8	686 ± 32	0.64

in the fit due to the deterioration in the signal (note that the summed ratios display smooth behavior up to $t = 17a$). The results, detailed in Table I, are compatible with those for the summed ratios.

Turning to the GEVP-improved summed ratios (again with $c = 2a$, $t \geq 4a$), we find that the excited state contributions are sufficiently suppressed to employ the linear fit *Ansatz* (18) starting from $t = 4a$. The final results for the weighted averages for basis $\mathbb{B}_2$ are

$$\begin{aligned} g_S^{\mathrm{lat},u+d} &= 30.1 \pm 1.8\ [1.0, 0.8, 1.0] \\ g_S^{\mathrm{lat},s} &= 11.7 \pm 0.7\ [1.0, 1.2, 1.3]. \end{aligned} \tag{20}$$

The $\chi^2/\mathrm{N_{df}}$ for the three fits which enter the average (with fit ranges $t/a = 4$–11, $t/a = 5$–11 and $t/a = 6$–11) are given in brackets. For $\mathbb{B}_3$, we obtain

$$\begin{aligned} g_S^{\mathrm{lat},u+d} &= 30.3 \pm 1.8\ [1.1, 0.8, 1.1] \\ g_S^{\mathrm{lat},s} &= 11.6 \pm 0.9\ [1.1, 0.9, 1.2] \end{aligned} \tag{21}$$

for the same fit ranges. These four fit results for the charges are displayed as the green bands in Fig. 2. The standard and GEVP summed ratios are shown in Fig. S3 of the Supplemental Material [31], along with representative fits utilising Eqs. (17) and (18).

Summary and discussion. We utilised the variational approach with a basis including nucleon-sigma type interpolators to remove the dominant excited state contamination from the three-point correlation functions with a scalar current. The scalar charges are reliably extracted from source-sink separations $t \leq 1.1$ fm. The results of the standard method (Table I) agree well with the GEVP-improved numbers (20) and (21), however, the former require larger time separations (see also the comparison in Fig. 2). Considering the exponential increase in the noise over signal with t, we find the new method to be cost effective. Converting our values via Eqs. (8) and (9) into the σ-terms, we obtain $\sigma_{\pi N} = (235 \pm 24)$ MeV and $\sigma_{sN} = (42 \pm 16)$ MeV, where the large uncertainty, in particular for σ_{sN}, is mostly due to the large value of r_m at our coarse lattice spacing $a \approx 0.098$ fm ($r_m \approx 3.4$ [34]). The results are consistent with those at similar pion masses from other works [8,10,42].

For physical quark masses, the σ meson becomes unstable and one might be tempted to perform a full scattering analysis [43–49], including $N\pi\pi$ type interpolators. However, since the width of the $f_0(500)$ is similar to its energy [50], also a scalar bilinear interpolator will most likely couple well to the scattering states [32,33,51], as well as to the local isoscalar current. Therefore, the method presented here may very well be directly applicable to the physical point. Future studies with closer to physical pion masses will shed further light on this.

Acknowledgments. We thank P. Petrak for sharing results on the sigma terms with us. L. B. is grateful to his colleagues at DESY and at the Humboldt University for stimulating discussions, with special thanks to J. Green and R. Sommer for their insightful comments. He also extends his gratitude to R. Gupta and K.-F. Liu and the members of the χQCD collaboration for useful discussions. G. B. thanks S. Leupold for discussions. L. B. received support through the German Research Foundation (DFG) research unit FOR5269 "Future methods for studying confined gluons in QCD." Simulations were performed on the QPACE 3 computer of SFB/TRR-55, using an adapted version of the CHROMA [52] software package.

Data availability. The data that support the findings of this article are not publicly available upon publication because it is not technically feasible and/or the cost of preparing, depositing, and hosting the data would be prohibitive within the terms of this research project. The data are available from the authors upon reasonable request.

[1] J. M. Alarcón, Eur. Phys. J. Special Topics **230**, 1609 (2021).
[2] J. Gasser, H. Leutwyler, and M. E. Sainio, Phys. Lett. B **253**, 252 (1991).
[3] M. Hoferichter, J. Ruiz de Elvira, B. Kubis, and U.-G. Meißner, Phys. Lett. B **843**, 138001 (2023).
[4] J. M. Alarcón, J. M. Camalich, and J. A. Oller, Phys. Rev. D **85**, 051503 (2012).
[5] Y.-H. Chen, D.-L. Yao, and H. Q. Zheng, Phys. Rev. D **87**, 054019 (2013).
[6] M. Hoferichter, J. Ruiz de Elvira, B. Kubis, and U.-G. Meißner, Phys. Rev. Lett. **115**, 092301 (2015).
[7] J. Ruiz de Elvira, M. Hoferichter, B. Kubis, and U.-G. Meißner, J. Phys. G **45**, 024001 (2018).
[8] Y.-B. Yang, A. Alexandru, T. Draper, J. Liang, and K.-F. Liu (χQCD Collaboration), Phys. Rev. D **94**, 054503 (2016).
[9] G. S. Bali, S. Collins, D. Richtmann, A. Schäfer, W. Söldner, and A. Sternbeck (RQCD Collaboration), Phys. Rev. D **93**, 094504 (2016).
[10] N. Yamanaka, S. Hashimoto, T. Kaneko, and H. Ohki (JLQCD Collaboration), Phys. Rev. D **98**, 054516 (2018).
[11] R. Gupta, S. Park, M. Hoferichter, E. Mereghetti, B. Yoon, and T. Bhattacharya, Phys. Rev. Lett. **127**, 242002 (2021).
[12] A. Agadjanov, D. Djukanovic, G. von Hippel, H. B. Meyer, K. Ottnad, and H. Wittig, Phys. Rev. Lett. **131**, 261902 (2023).
[13] C. Alexandrou, S. Bacchio, J. Finkenrath, C. Iona, G. Koutsou, Y. Li, and G. Spanoudes, arXiv:2412.01535.
[14] C. Alexandrou, V. Drach, K. Jansen, C. Kallidonis, and G. Koutsou, Phys. Rev. D **90**, 074501 (2014).
[15] S. Dürr *et al.* (Budapest-Marseille-Wuppertal Collaboration), Phys. Rev. Lett. **116**, 172001 (2016).
[16] S. Borsanyi, Z. Fodor, C. Hoelbling, L. Lellouch, K. K. Szabo, C. Torrero, and L. Varnhorst, arXiv:2007.03319.
[17] G. S. Bali, S. Collins, P. Georg, D. Jenkins, P. Korcyl, A. Schäfer, E. E. Scholz, J. Simeth, W. Söldner, and S. Weishäupl (RQCD Collaboration), J. High Energy Phys. 05 (2023) 035.
[18] B. Hu, X. Jiang, K.-F. Liu, P. Sun, and Y.-B. Yang (CLQCD Collaboration), arXiv:2411.18402.
[19] Y. Aoki *et al.* (Flavour Lattice Averaging Group (FLAG)), arXiv:2411.04268.
[20] H. W. Hamber, E. Marinari, G. Parisi, and C. Rebbi, Nucl. Phys. **B225**, 475 (1983).
[21] G. P. Lepage, in *From Actions to Answers. Proceedings, Theoretical Advanced Study Institute in Elementary Particle Physics, Boulder, CO, USA, 1989*, edited by T. A. DeGrand and D. Toussaint (World Scientific, Singapore, 1990), p. 97.
[22] B. C. Tiburzi, Phys. Rev. D **80**, 014002 (2009).
[23] O. Bär, Phys. Rev. D **94**, 054505 (2016).
[24] O. Bär, Phys. Rev. D **99**, 054506 (2019).
[25] O. Bär and H. Colic, Phys. Rev. D **103**, 114514 (2021).
[26] G. S. Bali, L. Barca, S. Collins, M. Gruber, M. Löffler, A. Schäfer, W. Söldner, P. Wein, S. Weishäupl, and T. Wurm (RQCD Collaboration), J. High Energy Phys. 05 (2020) 126.
[27] Y.-C. Jang, R. Gupta, T. Bhattacharya, B. Yoon, and H.-W. Lin (PNDME Collaboration), Phys. Rev. D **109**, 014503 (2024).
[28] L. Barca, G. Bali, and S. Collins, Phys. Rev. D **107**, L051505 (2023).
[29] C. Alexandrou, G. Koutsou, Y. Li, M. Petschlies, and F. Pittler, Phys. Rev. D **110**, 094514 (2024).
[30] M. Bruno *et al.* (CLS Effort), J. High Energy Phys. 02 (2015) 043.
[31] See Supplemental Material at http://link.aps.org/supplemental/10.1103/PhysRevD.111.L031505 for more details.
[32] C. B. Lang, L. Leskovec, M. Padmanath, and S. Prelovsek, Phys. Rev. D **95**, 014510 (2017).
[33] A. L. Kiratidis, W. Kamleh, D. B. Leinweber, Z.-W. Liu, F. M. Stokes, and A. W. Thomas, Phys. Rev. D **95**, 074507 (2017).
[34] J. Heitger, F. Joswig, P. L. J. Petrak, and A. Vladikas, Eur. Phys. J. C **81**, 606 (2021); Eur. Phys. J. C **82**, 104(E) (2022).
[35] J. Bulava, M. Donnellan, and R. Sommer, J. High Energy Phys. 01 (2012) 140.
[36] S. Güsken, U. Löw, K. H. Mütter, R. Sommer, A. Patel, and K. Schilling, Phys. Lett. B **227**, 266 (1989).
[37] S. Güsken, Nucl. Phys. B Proc. Suppl. **17**, 361 (1990).
[38] M. Falcioni, M. L. Paciello, G. Parisi, and B. Taglienti, Nucl. Phys. **B251**, 624 (1985).
[39] L. Maiani, G. Martinelli, M. L. Paciello, and B. Taglienti, Nucl. Phys. **B293**, 420 (1987).
[40] R. Sommer, Nucl. Phys. B, Proc. Suppl. **42**, 186 (1995).
[41] M. Foster and C. Michael (UKQCD Collaboration), Phys. Rev. D **59**, 094509 (1999).
[42] P. L. J. Petrak, G. Bali, S. Collins, J. Heitger, D. Jenkins, and S. Weishäupl, Proc. Sci. LATTICE2022 (**2023**) 112 [arXiv:2301.03871].
[43] R. A. Briceño, J. J. Dudek, R. G. Edwards, and D. J. Wilson (for the Hadron Spectrum Collaboration), Phys. Rev. Lett. **118**, 022002 (2017).
[44] L. Liu *et al.* (ETM Collaboration), Phys. Rev. D **96**, 054516 (2017).
[45] Z. Fu and X. Chen, Phys. Rev. D **98**, 014514 (2018).
[46] D. Guo, A. Alexandru, R. Molina, M. Mai, and M. Döring, Phys. Rev. D **98**, 014507 (2018).
[47] T. Blum *et al.* (RBC and UKQCD Collaborations), Phys. Rev. D **107**, 094512 (2023); Phys. Rev. D **108**, 039902(E) (2023).
[48] A. Rodas, J. J. Dudek, and R. G. Edwards (Hadron Spectrum Collaboration), Phys. Rev. D **108**, 034513 (2023).
[49] M. Bruno, D. Hoying, T. Izubuchi, C. Lehner, A. S. Meyer, and M. Tomii, arXiv:2304.03313.
[50] S. Navas *et al.* (Particle Data Group), Phys. Rev. D **110**, 030001 (2024).
[51] D. Severt, M. Mai, and U.-G. Meißner, J. High Energy Phys. 04 (2023) 100.
[52] R. G. Edwards and B. Joó (SciDAC, LHP and UKQCD Collaborations), Nucl. Phys. B, Proc. Suppl. **140**, 832 (2005).